Journal of Achievements in Materials and Manufacturing Engineering
VOLUME 31
ISSUE 2
December
2008

Analysis of the precipitation and growth processes in a high-temperature Fe–Ni alloy

K.J. Ducki*
Materials Science Department, Silesian University of Technology,
ul. Krasińskiego 8, 40-019 Katowice, Poland
* Corresponding author: E-mail address: kazimierz.ducki@polsl.pl

Received 07.10.2008; published in revised form 01.12.2008

Materials

ABSTRACT

Purpose: The influence of prolonged aging on the precipitation process of the intermetallic phases, carbide and boride in high-temperature Fe–Ni austenitic alloy has been studied. Taking advantage of the LSW theory, at attempt was undertaken to provide a quantitative description of the γ' phase particles growth as a function of temperature and aging time.
Design/methodology/approach: The samples were subjected to a solution heat treatment at 980°C/2h/water, and then aged at 715, 750 and 780°C, with holding times 0.5–500 h. Structural investigations were conducted using transmission electron microscopy (TEM) and X-ray diffraction.
Findings: Direct measurements on the electron micrographs allowed to calculate the structural parameters of the γ' phase: mean diameter, volume fraction and mean distance between particles. In accordance with the LSW theory, linear dependencies of changes in mean diameter as a function of $t^{1/3}$ were elaborated and the activation energy (E) of the γ' phase coagulation process was determined.
Practical implications: The obtained data of γ' phase particles growth as a function of temperature and aging time can be used to evaluate the degree of Fe–Ni alloys structure degradation and the distributions of temperatures during their operation at high temperatures.
Originality/value: The paper touches upon the problem of the development of modern quantitative metallography methods with the use of thin foil technique and using theory LSW to describe a growth and coagulation processes of particles γ' phase in high-temperature Fe–Ni alloy.
Keywords: Metallic alloys; Heat treatment; Precipitation and coagulation; LSW theory

1. Introduction

Precipitation strengthened heat resistant Fe–Ni austenitic alloys achieve their optimum properties after multi-stage heat treatment consisting of solution treatment (or annealing) and various methods of aging. During preliminary heat treatment, the precipitation processes take place of γ'[Ni_3(Al,Ti)] and G [$Ni_{16}Ti_6Si_7$] intermetallic phases, as well as the carbide $M_{23}C_6$ and boride M_3B_2 [1-5]. During prolonged aging or utilization at elevated temperatures, processes of coagulation of γ' phase and overaging take place in Fe–Ni alloys [6-9]. The process of γ' phase particles growth can be described by means of the LSW (Lifshitz–Slyozov–Wagner) coagulation theory [10,11].

In the present paper the influence of prolonged aging on the course of precipitation and coagulation of γ' phase in the A-286 type high-temperature austenitic alloy was investigated. The basic stereological parameters of the γ' phase particles have been determined and the growth step of the γ' phase has been analyzed on the basis of the LSW theory.

2. Material and procedure

Rolled bars, 16 mm in diameter, of an austenitic Fe–Ni alloy designated X5NiCrTi26-15 were studied. The chemical composition of the material is given in Table 1.

The samples for testing cut off these rods were subjected to solution heat treatment at 980°C for 2 h and water quenched, and then aged at temperatures 715, 750 and 780°C at holding time from 0.5 to 500 h.

The structural examinations were carried out using the thin foil technique on a Jeol JEM-2000 FX transmission electron microscope (TEM). The X-ray phase analysis of isolates was performed on a Philips PW-1140 X-ray diffractometer.

A quantitative analysis of secondary γ' phase particles, which phase precipitated in the alloy during ageing, was performed on TEM images in bright field mode. Based on direct counting, basic stereological parameters of the γ' phase were determined from binary images, i.e.: the mean diameter ($\overline{D}$), the volume fraction particles (V_V) and the mean distance between particles (l_d).

The mean diameter ($\overline{D}$) of the particles was evaluated with help of the relation given by [13,14].

$$\overline{D} = \frac{\overline{d}t}{t - \overline{d} + \left(\pi A_A / L_A\right)} \tag{1}$$

where: $\overline{d}$ – the mean diameter of the circles in the projected plane (nm), t – the foil thickness (nm), A_A – the projection area, L_A – the perimeter density (1/nm).

The volume fraction (V_V) of γ' particles was calculated using the formula provided by [14]:

$$V_V = \frac{\pi}{6}\frac{\sum N_i d_i^3}{A\left(t + \overline{d}\right)} \tag{2}$$

where: N_i – the number of particles with diameter d_i, A – the total projection area (nm^2).

The mean distance between particles (l_d) was calculated by means of an equation given by [16]:

$$l_d = \overline{d}\sqrt{\frac{\pi}{6V_V}\left(1 + \frac{s^2}{\overline{d}^2}\right)} - \frac{\pi}{4}\overline{d} \tag{3}$$

where: s-the standard deviation of the particle diameter distribution.

The analysis of the γ' phase growth step was made on the basis of the LSW theory for coagulation on volume diffusion controll according to the relationship provided by [12].

$$\overline{d}^3 - \overline{d}_0^3 = \frac{64\sigma D C_e V_m^2}{9RT} = K't \tag{4}$$

where: $\overline{d}$ and $\overline{d}_0$ - average diameter of precipitates at time t and t = 0 respectively, σ - the interfacial energy between precipitates and matrix, D - the diffusion coefficient of the solute atom in the matrix, C_e - the concentration of solute atoms in the matrix in equilibrium with a particle of an infinite size, V_m - the molar volume of precipitation phase, R - the gas constant, T - the absolute temperature, K' – the growth rate constant.

In general the diffusion coefficient (D) is expressed as:

$$D = D_0 \cdot \exp\left(-E/RT\right) \tag{5}$$

where D_0 – is the pre-exponential factor, E – is the activation energy of diffusion.

Therefore, the K' constant in Equation (4) takes on the following form:

$$K' = \frac{64\sigma D_0 C_e V_m^2 \exp\left(-E/RT\right)}{9RT} \tag{6}$$

where D_0 – is the pre-exponential factor, E – is the activation energy of diffusion.

On assumption that the values of σ, C_e and V_m are nearly independent of temperature, the value of diffusion activation energy (E) can be obtained from the slope of Arrhenius plot being the linear relationship between ln(TK') and T^{-1}.

3. Experimental results

After solution heat treatment at 980°C/2h/water, the investigated Fe–Ni alloy has the structure of twinned austenite with an elevated density of dislocations and about 0.3 wt.% of undissolved precipitates (Fig. 1).

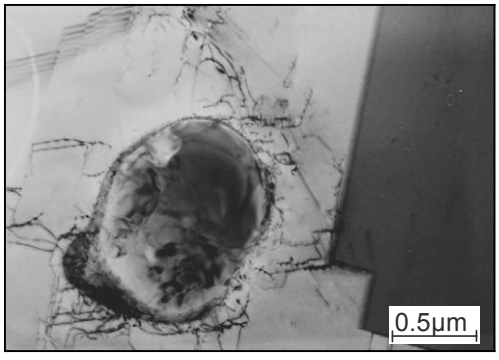

Fig. 1. Structure of the alloy after solution heat treatment at 980°C/2h/w. Twinned austenite with increased dislocation density and undissolved particle of $Ti_4C_2S_2$

Table 1.
Chemical composition of the investigated Fe–Ni alloy

Content of an element (wt.%)														
C	Si	Mn	S	P	Cr	Ni	Mo	W	V	Ti	Al	Co	B	N
0.050	0.55	1.25	0.016	0.026	14.3	24.5	1.34	0.10	0.41	1.88	0.16	0.08	0.007	0.0062

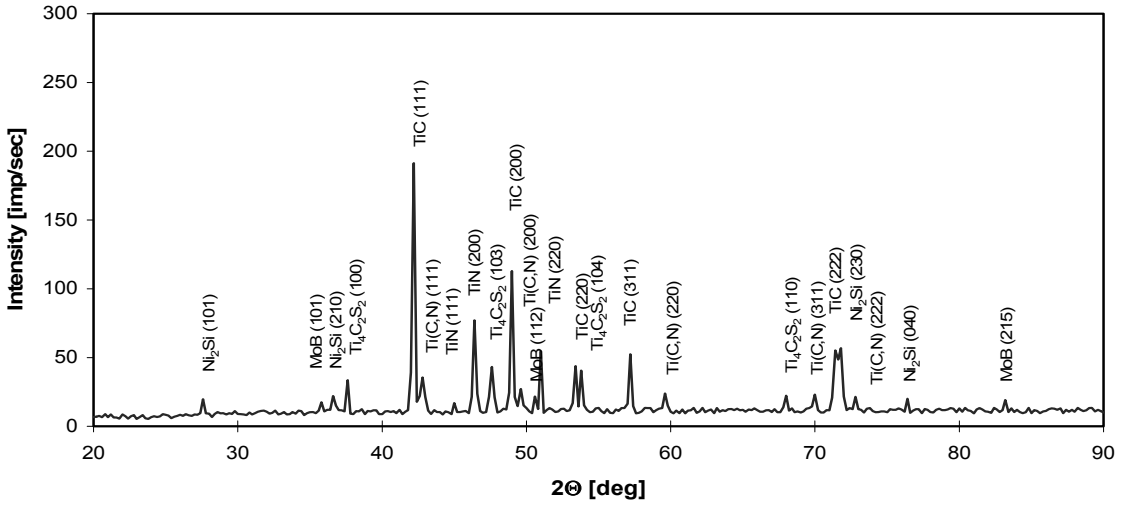

Fig. 2. X-ray diffraction pattern of alloy izolate after solution heat treatment at 980°C/2h/water

The appearance of titanium compounds, i.e. carbide TiC, nitride TiN, carbonitride Ti(C,N), carbosulfide $Ti_4C_2S_2$ and Laves phase Ni2Si and boride MoB, was found in the extracted precipitates (Fig. 2).

The application of single-stage aging after solutioning at 715, 750 and 780°C for 0.5-500 h initiates the precipitation processes of intermetallic phases, carbide and boride (Figs. 3-8). At initial stages of aging at a temperature 715°C a precipitation process of fine flakes of G [$Ni_{16}Ti_6Si_7$] phase at the grain boundaries occurred (Fig. 3).

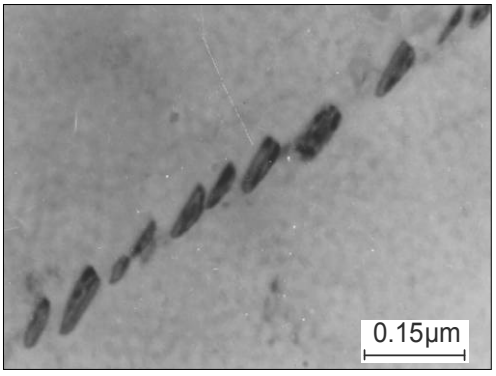

Fig. 3. Structure of the alloy after solution heat treatment and aging at 715°C/8h. Fine flakes of G phase at a grain boundary and coherent zones in the matrix

Early stages of the creation of coherent zones rich in Ti and Al were observed within the austenite grains which, according to [17], is connected with spinodal decomposition of the supersaturated austenite. The main phase precipitating during alloy aging was the γ' [Ni_3(Al,Ti)] intermetallic phase, which precipitated homogeneusly in the form of dispersive particles coherent with the matrix (Fig. 4).

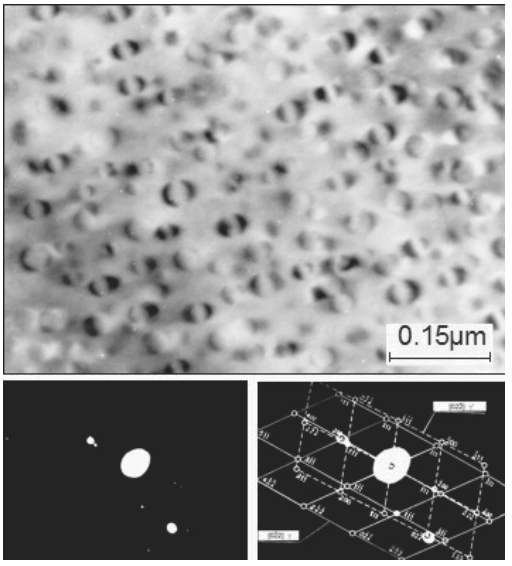

Fig. 4. Structure of the alloy after solution heat treatment and aging at 715°C/150h. Coherent spheroidal γ' phase precipitates in the matrix

An increase of aging temperature up to 750°C intensifies diffusion processes of the γ' phase particles growth and coagulation (Fig. 5). The structure of alloy shows also first effects of overaging into form of transcrystalline Widmanstätten plates of the η [Ni_3Ti] phase (Fig. 6). The phase transition γ'→ η appeared in the austenite areas and was accompanied by a dissolution of the neighbouring γ' phase particles in the matrix.

At the highest aging temperature of 780°C, the alloy structure demonstrated visible effects of overaging connected with the coagulation of γ' phase particles (Fig. 7). The cellular η phase nucleated at a vicinity of grain boundary of matrix by celluar reaction and grew up in clusters (Fig. 8).

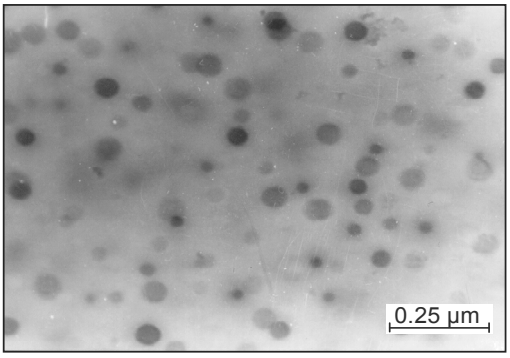

Fig. 5. Structure of the alloy after solution heat treatment and aging at 750°C/300h. Diversified size of spheroidal γ' phase particles in the matrix

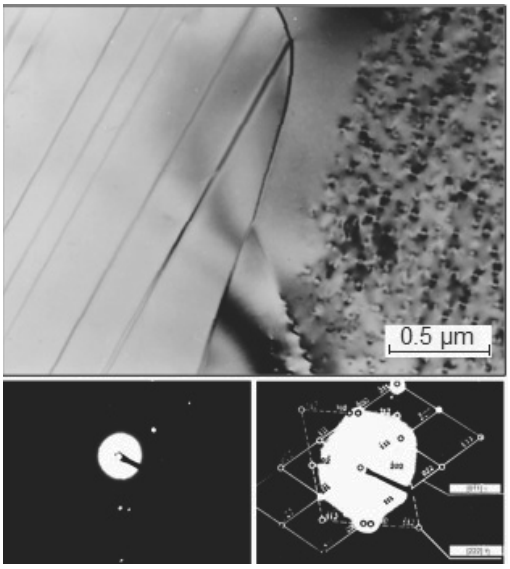

Fig. 6. Structure of the alloy after solution heat treatment and aging at 750°C/100h. The transcrystalline plates of the η phase in the matrix

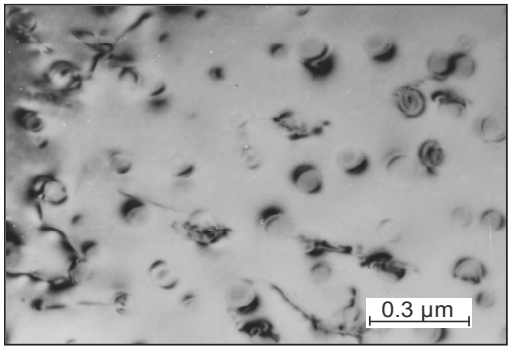

Fig. 7. Structure of the alloy after solution heat treatment and aging at 780°C/500h. Coagulated spheroidal γ' phase particles in the matrix

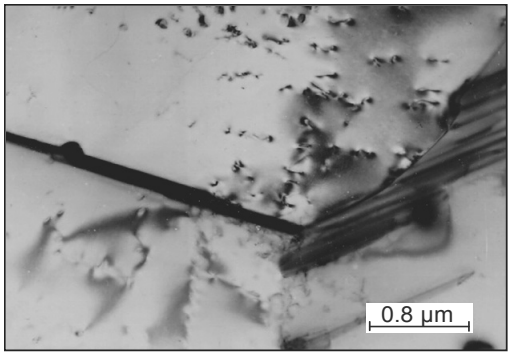

Fig. 8. Structure of the alloy after solution heat treatment and aging at 780°C/500h.Celluar precipitates of the η phase in the zone near grain boundary

X-ray examinations of the sample isolates after aging showed the appearance of the same phases as those observed in the supersaturated state, i.e. TiC, TiN, Ti(C,N), $Ti_4C_2S_2$, Ni_2Si and MoB. Besides, in aged alloy often the following phases were discovered: γ'[Ni_3(Al,Ti)], G phase [$Ni_{16}Ti_6Si_7$], η phase [Ni_3Ti], β phase [NiTi], carbide $M_{23}C_6$ and boride M_3B_2 (Figs. 9-11).

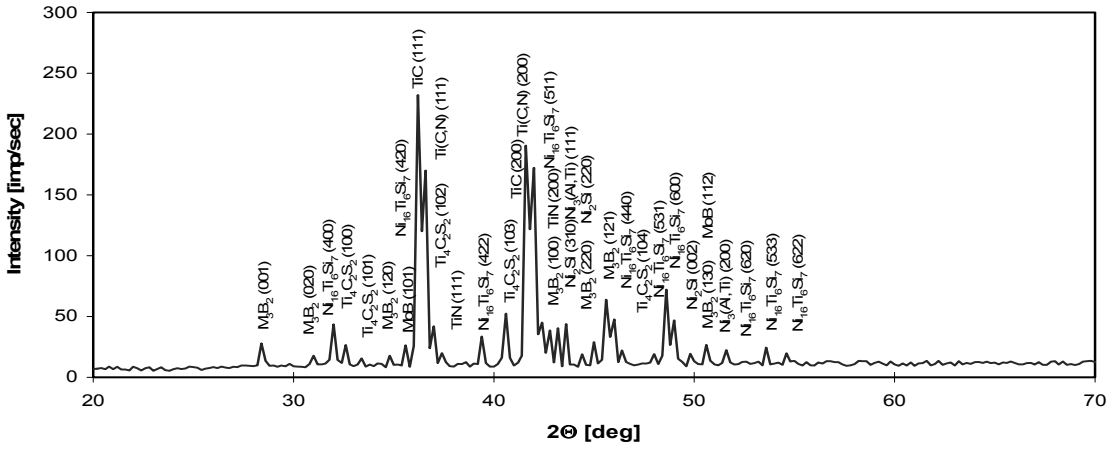

Fig. 9. X-ray diffraction pattern of alloy izolate after solution heat treatment and aging 715°C/150h

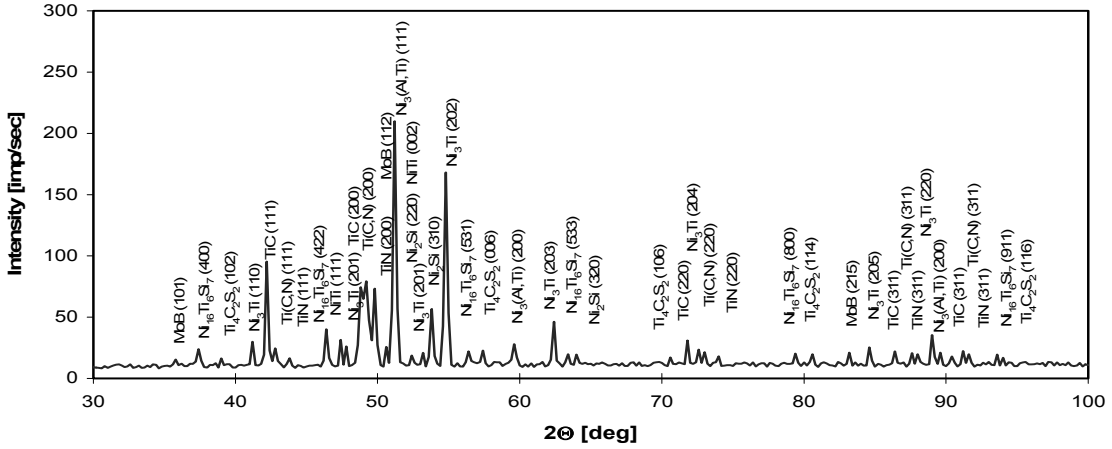

Fig. 10. X-ray diffraction pattern of alloy izolate after solution heat treatment and aging 750°C/300h

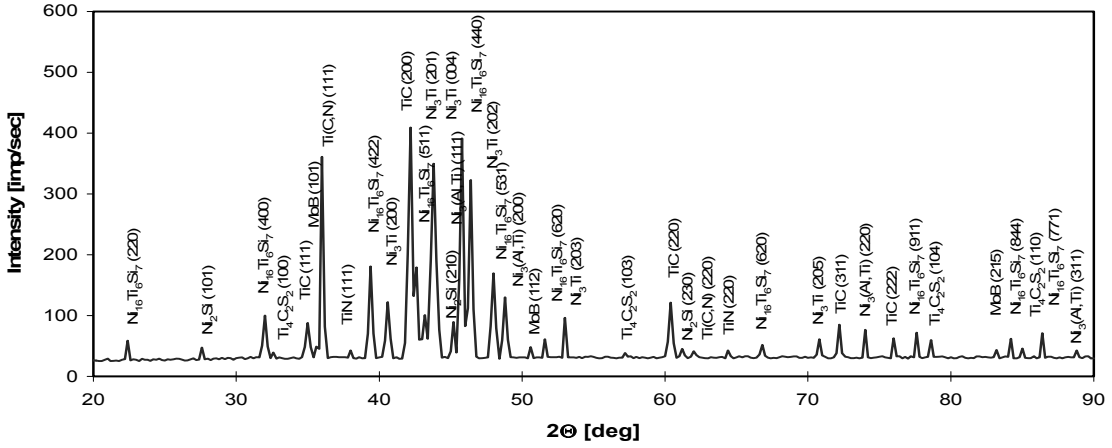

Fig. 11. X-ray diffraction pattern of alloy izolate after solution heat treatment and aging 780°C/500h

Table 2.
Stereological parameters of the γ' particles in the tested Fe–Ni alloy

Stereological parameters	Time of aging (h) at 715°C					Time of aging (h) at 750°C					Time of aging (h) at 780°C				
	4	50	150	300	500	4	50	150	300	500	4	50	150	300	500
A_A (%)	2.1	6.0	16.5	9.8	10.9	3.2	17.7	11.5	13.3	15.6	5.6	5.3	11.5	10.0	9.5
$\overline{d}$ (nm)	7.4	10.5	25.7	18.7	19.9	9.2	18.9	24.3	28.6	36.6	12.7	24.3	47.2	53.6	70.7
$\overline{D}$ (nm)	7.5	11.4	17.1	21.5	23.0	10.6	20.6	28.8	34.3	45.1	13.1	25.1	52.5	62.3	85.9
V_V (%)	0.07	0.3	1.0	1.1	1.4	0.1	1.2	1.1	1.5	2.1	0.4	2.3	7.7	7.8	8.4
l_d (nm)	195	144	106	127	121	217	115	128	155	164	153	103	89	103	124

The quantitative analysis of γ' phase particles precipitating in the alloy during aging was carried out at for aging temperatures of 715, 750 and 780°C and holding times from 4 to 500 hrs. Table 2 provides the results of quantitative examinations obtained for selected times of aging, i.e.: 4, 50, 150, 300 and 500 h. As can be seen from the data provided, at aging temperature of 715°C and holdings times from 4 to 500h, the mean diameter of particles ($\overline{D}$) increased from 7.5 to 23 nm, whereas the particles' volume fraction changed in a small scope of 0.07 to 1.4%. At a higher aging temperature of 750°C and the same holdings times, a growth of the average diameter of particles from 10.6 to 45.1 nm was observed together with a change in volume fraction from 0.1 to 2.1%.

At the highest aging temperature of 780°C and analogical holding times, the average diameter of particles reached the highest values in the scope of 13.1-85.9 nm, also with the highest volume fraction in the range between 0.4 and 8.4%. Exemplary histograms of the particle distributions for selected aging times from 4 to 500 h at temperature 715-780°C are presented in Figs. 12-15. With increasing aging time and temperature, a shift of the maximum toward the classes of larger diameter is noted. This confirms an

increasing mean diameter ($\overline{D}$) of γ' particles along with the prolongation of aging time and raiseing of aging temperature.

The growth process of γ' phase particles in the examined Fe–Ni alloy was analyzed using the LSW theory according to Equation (4) given by [12]. The relationship between the mean diameter of precipitates ($\overline{D}$) and the cube root of the aging time is presented in Fig. 16. For the analyzed aging temperatures, the obtained relationships are linear, which proves the fact that coagulation of γ' phase particles proceeds in accordance with the LSW theory and is controlled by volume diffusion. The slopes of curves increase with the increase of aging temperatures, which may be justified with a higher coagulation rate for γ' phase particles.

The activation energy of the γ' phase coagulation process in the examined Fe–Ni alloy was determined from the Arrhenius straight line slope (Fig. 17). The value obtained (E = 299 kJ/mole) is close to the value of activation energy (283 kJ/mole) determined for the A-286 alloy by [12].

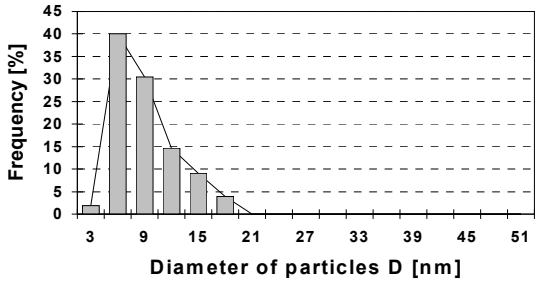

Fig. 12. Size distribution of the γ' particles in the alloy after solution heat treatment and aging 715°C/4h

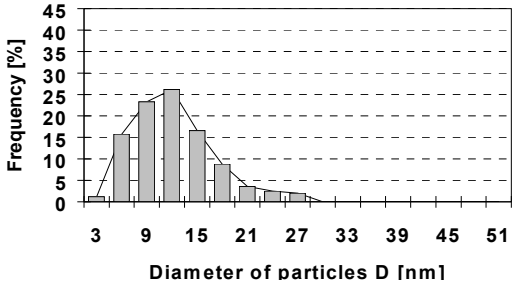

Fig. 13. Size distribution of the γ' particles in the alloy after solution heat treatment and aging 715°C/50h

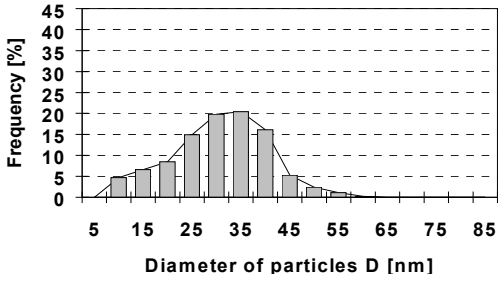

Fig. 14. Size distribution of the γ' particles in the alloy after solution heat treatment and aging 750°C/150h

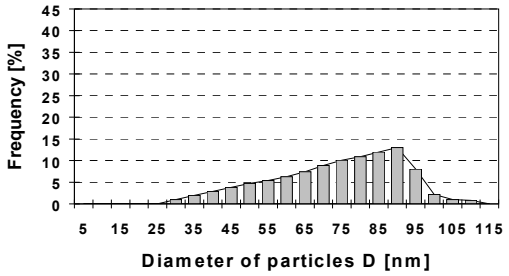

Fig. 15. Size distribution of the γ' particles in the alloy after solution heat treatment and aging 780°C/500h

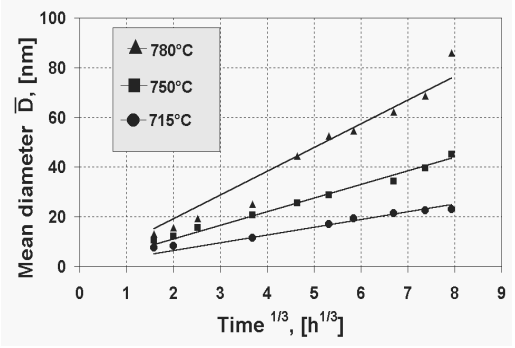

Fig. 16. Relationship between the mean diameter of γ' phase particles and the cube root of aging time at temperatures of 715, 750 and 780°C

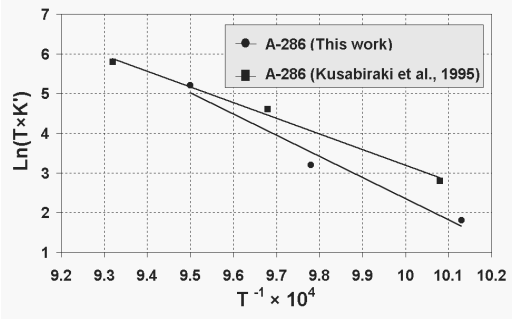

Fig. 17. Arrhenius plots for determination of the activation energy for growth of γ' phase precipitates in the examined Fe–Ni alloy and in the A-286 alloy [12]

4. Summary

The performed inspections and analysis of results had disclosed an important influence of prolonged aging in elevated temperatures on the substructure of high-temperature Fe–Ni austenitic alloy of A-286 type.

The investigated Fe–Ni alloy after solution heat treatment at 980°C/2h/water is characterized by a structure of twinned austenite with a small amount (ca. 0.3 wt.%) of undissolved

precipitates of titanium compounds, i.e. carbide TiC, nitride TiN, carbonitride Ti(C,N), carbosulfide $Ti_4C_2S_2$, Laves' phase Ni_2Si and boride MoB.

The application of a single-stage aging, after solution heat treatment, at temperatures of 715, 750 and 780°C, with holding times from 0.5 to 500 h, causes precipitation processes of γ', η, β and G intermetallic phases in the investigated alloy, as well as the carbide $M_{23}C_6$ and boride M_3B_2.

The main phase precipitating during alloy aging was the γ' intermetallic phase. During the precipitation of the γ' phase one may distinguish three characteristic stages, i.e. coherent zones, coherent spheroidal particles (10-35 nm) and coagulated spheroidal particles (40-85 nm). The obtained histograms of the size distribution of the γ' phase shows a shift of the maximum toward the classes of larger diameter with increasing aging time and temperature. The volume fraction of γ' phase particles was dependent on the temperature and aging time and changed within the scope of ca. 0.1% to 8.4%.

It was found that the mean diameter of γ' phase precipitates increases as a function of the cube root of aging time, which is consistent with the predictions based on the LSW theory for the coagulation controlled by volume diffusion. The determined value of activation energy for the process of γ' phase coagulation in the examined alloy was 299 kJ/mole. This value was very close to the activation energy for diffusion of solute elements in γ-Fe which are considered to contribute to the growth of γ' phase.

The η phase had two types of precipitate shapes, i.e. Widmanstätten plates and celluar precipitates. Widmanstätten-like η phase nucleated in the matrix grain, whereas celluar η phase nucleated at the vicinity of austenite grain boundary.

Acknowledgements

This work was supported by the Committee of Scientific Research of Poland under grant No. 7 T08A 038 18.

References

[1] S. Asgari, Structure and strain hardening of superalloy AEREX 350, Journal of Materials Processing Technology 118 (2001) 246-250.
[2] H.S. Jeong, J.R. Cho, H.C. Park, Microstructure prediction of Nimonic 80A for large exhaust valve during hot closed dieforging, Journal of Materials Processing Technology 162-163 (2005) 504-511.
[3] P. Jonsta, Z. Jonsta, J. Sojka, L. Cizek, A. Hernas, Structural characteristics of nickel super alloy INCONEL 713LC after heat treatment, Journal of Achievement in Materials and Manufacturing Engineering 21/2 (2007) 29-32.
[4] M. Konter, M. Thumann, Materials and manufacturing of advanced industrial gas turbine components, Journal of Materials Processing Technology 117 (2001) 386-390.
[5] K.J. Ducki, Precipitation and growth of intermetallic phase in a high-temperature Fe–Ni alloy, Journal of Achievements in Materials and Manufacturing Engineering 18 (2006) 87-90.
[6] S.A. Sajjadi, S.M. Zebarjad, Study of fracture mechanisms of a Ni-Base superalloy at different temperatures, Journal of Achievements in Materials and Manufacturing Engineering 18 (2006) 227-230.
[7] R. Shargi-Moshtaghin, S. Asgari, The influence of thermal exposure on the γ' precipitates characteristics and tensile behaviour of superalloy IN-738LC, Journal of Materials Processing Technology 147 (2004) 343-350.
[8] J.M. Zhang, Z.Y. Gao, J.Y. Zhuang, Z.Y. Zhong, Grain growth model of IN718 during holding period after hot deformation, Journal of Materials Processing Technology 101 (2000) 25-30.
[9] I.M. Lifshitz, V.V. Slyozow, The kinetics of precipitation from supersaturated solid solution, Journal of Physics and Chemistry of Solids 19 (1961) 35-50.
[10] C. Wagner, Theory of transformation in sludge throw theresolution, Journal of Electrocemic 65 (1961) 581-591 (in German).
[11] K. Kusabiraki, Y. Takasawa, T. Ooka, Precipitation and Growth of γ' and η Phases in 53Fe–26Ni–15Cr alloy, ISIJ International 35 (1995) 542-547.
[12] A. Czyrska-Filemonowicz, B. Dubiel, K. Wiencek, Determination of the oxide particle density in ODS alloys means of transmission electron microscopy, Acta Stereologica 17/2 (1998) 225-236.
[13] A. Wasilkowska, M. Bartsch, U. Messerschmidt, R. Herzog, A. Czyrska-Folemonowicz, Creep mechanisms of ferritic strengthened alloys, Journal of Materials Processing Technology 133 (2003) 218-224.
[14] B. Dubiel, J. Wosik, H.J. Penkalla, A. Czyrska-Filemonowicz, Quantitative TEM microstructural analysis of Ni-based superalloy Waspaloy, Proceedings of the Stereology and Image Analysis in Materials Science, Kraków, 2000, 135-140.
[15] J.H. Schröder, E. Arzt, Electron-Microscopic investigation of dispersion-strengthened superalloys, Praktische Metallography 25 (1988) 264-273.
[16] F.B. Pickering, Some aspects of the precipitation of nickel–aluminium–titanium intermetallic compounds in ferrous materials, Proceedings of the International Conference "The metallurgical evolution of stainless steels", London, 1979, 391-401.
[17] K.J. Ducki, Analysis of the structure and precipitation strengthening in a creep resisting Fe-Ni alloy, Journal of Achievement in Materials and Manufacturing Engineering 21/2 (2007) 25-32.